Three dimensional knot models based on surface laser scanning

Andreas Briggert
Dept. of Building Technology, Linnaeus University, Växjö, Sweden, andreas.briggert@lnu.se

Anders Olsson
Dept. of Building Technology, Linnaeus University, Växjö, Sweden, anders.olsson@lnu.se

Jan Oscarsson
Dept. of Building Technology, Linnaeus University, Växjö, Sweden, jan.oscarsson@lnu.se

Abstract

Most machine strength grading methods of today result in limited grading accuracy and poor yield in higher strength classes. A new and more accurate grading method utilizing laser scanning technique to determine the in-plane fibre directions on board surfaces was recently approved for the European market. In this, however, no consideration is taken to the out-of-plane direction of the fibres. A first step towards scanning-based 3D models of the fibre orientation is the establishment of 3D knot models. In this investigation laser scanning was used to identify knot surfaces on longitudinal board surfaces. By means of developed algorithms knot surfaces that belonged to the same physical knot visible on different sides of the board were identified. All knots with surface areas larger than 100 mm^2 were correctly identified and modeled in 3D. This is a promising starting point for further development of the new grading method based on laser scanning.

Keywords: structural timber, knots, laser scanning, tracheid effect, local fibre direction, diving angle

Introduction

Background

Destructive testing of structural timber typically results in the conclusion that failures are strongly related to the occurrence of knots. For example, Johansson (2003) evaluated results from about 1800 boards tested in bending or tension and found that more than 90 % of the failures were connected to the existence of this kind of defects. On the contrary, other investigations highlight the fact that the statistical relationship between strength and *indicating properties* (IPs) reflecting size and position of knots is rather weak. The *coefficient of determination* (R^2) between such IPs and bending strength typically vary between 0.16–0.27 (Hoffmeyer 1995), which is poor in comparison with common grading methods in which *modulus of elasticity* (MoE) measures based on axial dynamic excitation or flatwise bending are applied as IPs. Such methods, which typically result in R^2 values of about 0.5 (Johansson 2003), utilize the fact that the best single predictor of strength is stiffness expressed in terms of different MoEs.

There is in a sense a contradiction between, on one hand, failure of timber being dependent on the occurrence of knots and, on the other hand, the statistical relationship between knot measures and strength being poor. However, this can be understood from the fact that failure in bending or tension is typically not initiated in an actual knot, but in adjacent clear wood areas where the fibre orientation deviates strongly from the longitudinal direction of the tested piece (e.g. Boughton 1994). Furthermore, Foley (2003) concluded that the strength reducing effect related to knots was most likely caused by a combination of *inter alia* fibre deviations and reduced area of clear wood in the cross-section. Thus, development and application of new IPs that include the strength- and stiffness-reducing effect of both knots and fibre deviations could be expected to be very useful in the development of new strength grading methods.

It is well known that dot laser scanning and utilization of the so called tracheid effect, see below, can be applied for the purpose of determining local fibre directions with high resolution on board surfaces (Åstrand 1996). Commercial equipment for laser scanning carried out at sawmill production speed has been available on the market for several years but it is not until very recently that such information has been used for strength grading purposes. A new grading method based on dot laser scanning using an optical scanner of make WoodEye (Innovativ Vision 2015), in combination with axial dynamic excitation and weighing using a grading machine of make Precigrader (Dynalyse 2015), was approved on the 3rd of March 2015 by the technical group TG1 set up under the technical committee TC 124 within the European Committee for Standardization. The method, which is presented in Olsson et al. (2013), is based on the fact that local fibre directions deviating from the longitudinal direction of a board result in a reduction of local stiffness in longitudinal board direction. By means of integration over cross-sections, a bending MoE profile is calculated across a board and the lowest local bending MoE found across this profile is used as IP. It has been shown that the new method will provide grading with high accuracy (Olsson et al. 2013; Oscarsson et al. 2014) in spite of the fact that the method, as approved, is based on several assumptions. For example, it is assumed that measured fibre directions are 1) located in the longitudinal-tangential plane, 2) valid to a certain depth, and 3) coinciding with the scanned board surface. The latter means that the so called diving angle, i.e. the out-of-plane angle, is set to zero, which it is not in reality. A further assumption is that the occurrence of knots is not considered, i.e. scanned fibres within knots are assumed to be clear wood fibres, but with directions that strongly deviate from the longitudinal board direction. Consequently, the intricate three-dimensional (3D) fibre pattern that occurs in the transition zone between knot and clear wood (Shigo 1997; Foley 2003) is neglected, although failures are frequently initiated in, or close to, such areas.

If the present two-dimensional (2D) fibre orientation model implemented in the grading method described in Olsson et al. (2013) was replaced by an accurate 3D fibre orientation model in which also the occurrence of knots was included, it is very likely that a further improvement of the relationship between IP and strength would be achieved. Such a fibre orientation model would also enable even more advanced calculations for assessment of strength, considering the development of cracks and fracture. The purpose of this paper is to initiate the development towards accurate knot and fibre orientation models in 3D.

Tracheid effect and determination of fibre direction

The in-plane fibre orientation on surfaces of softwood timber can be determined using the so called *tracheid effect*, which means that the tracheids (fibres) in softwood conduct concentrated light such as laser light better along the fibres than across. When a beam of such light illuminates a board, some of the light will penetrate the surface and scatter within the wood. A part of the scattered light will be reflected back to the surface and due to the tracheid effect the reflected light will take the shape of an ellipse with the major axis following the direction of the fibres at the surface. The left image in Figure 1a shows a softwood surface in which a knot is included; the right image displays the light scattering on the same surface when illuminated by dot lasers. By determining the major axis of each light spot the in-plane fibre orientation at the surface can be determined. Inside the knot, where the fibre direction is close to perpendicular to the surface, the fiber direction is determined more or less at random. This is a consequence of the fact that the shape of the ellipse becomes close to circular when fibres with a large diving angle are illuminated by a dot laser and, hence, making it difficult to determine the major axis of the ellipse that corresponds to in-plane direction of the fibre.

Methods based on the tracheid effect have also been developed for the purpose of determining the diving angle on board surfaces. Simonaho et al. (2004) suggested that the diving angle could be interpreted by a shape factor ratio determined as the ratio between the minor- and major axis of a reflected light spot. Olsson and Oscarsson (2014) used this in an attempt to model the 3D fibre orientation on the wide faces on sideboards of Norway spruce. The value of the diving angle (β) was calculated as

$$\beta = cos^{-1}\left(\left(\frac{l_1 + l_2}{2} - R\right)\frac{2}{l_2 - l_1}\right) \quad , \qquad l_1 < R < l_2 \tag{1}$$

where l_1 and l_2 are the ratios between the lengths of the minor- and major axis below and above which diving angles are assumed to be 0° and 90°, respectively, and R is the shape factor ratio of the studied ellipse. A consequence of this equation is that the more circular the ellipse, the higher the value of the diving angle. The mapping suggested by Olsson and Oscarsson (2014) for Norway spruce is shown in Figure 1b, in which the boundary values l_1 and l_2 are set to 0.54 and 0.82, respectively.

The theories presented above regarding determination of in-plane and out-of-plane angles must be adopted with caution when modelling fibre orientation in timber and there are two reasons for this. Firstly, in the 3D fibre orientation modelling carried out by in Olsson and Oscarsson (2014) the complicated 3D fibre pattern that occurs around knots, in the transition zone between knot and clear wood, was not captured accurately since no distinction between fibres that integrate with the knot and fibres that grow around the knot was made in the model. Thus, the result is not consistent with theories concerning growth such as Shigo's knot formation theory (Shigo 1997). Secondly, the mapping between the shape factor ratio and the diving angle, see Figure 1b, may be sensitive to the roughness and the colour of the wood surface. Still, however, the method is useful and reliable for certain purposes.

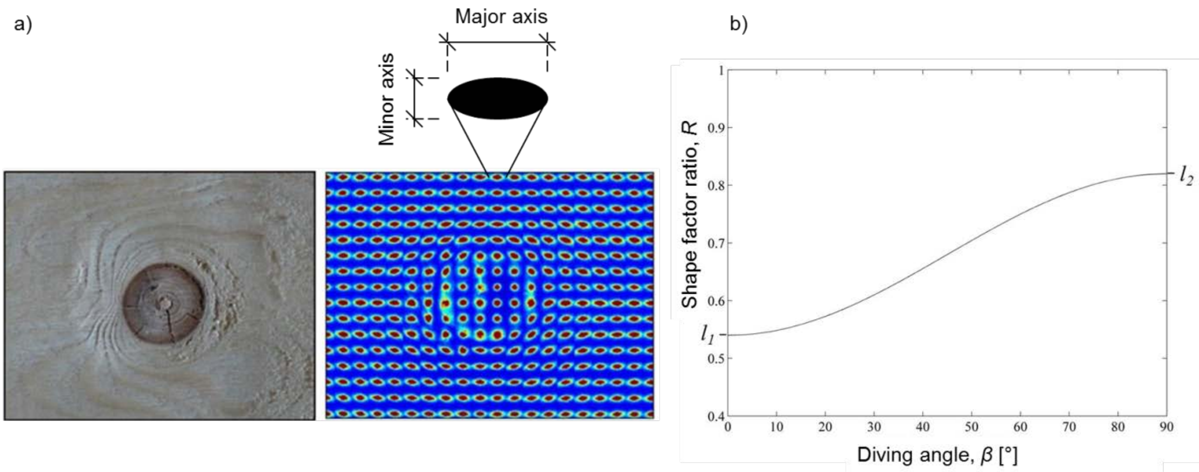

Figure 1— a) Left: surface of softwood timber including a knot. Right: spread of light (tracheid effect) due to dot laser illumination. Figure originates from Petersson (2010).
b) Mapping between shape factor ratio and value of the diving angle. Figure originates from Olsson and Oscarsson (2014).

Purpose, aims and limitations

The purpose of the present paper is to define a scheme for how models of the 3D orientation of knots in boards can be established on the basis of data from high speed laser scanning and utilization of the tracheid effect. Since the orientation of a knot is decisive for the orientation of fibres flowing around or integrating with it, the development of 3D knot models is regarded as an important step towards modelling the entire 3D fibre structure within a board. The aims of the present research are

- to determine positions and areas of knot surfaces visible on different sides of a board,
- to identify knot surfaces belonging to the same physical knot and create a complete 3D model of all knots within the board (knots smaller than 10 mm^2 are ignored).

Material and equipment

The test sample used in this study comprises in total 10 boards of Norway spruce with dimensions 45×145×4800 mm delivered from Södra Wood's sawmill in Torsås, Kalmar County, Sweden. All surfaces were planed prior to scanning but the planing was not satisfactory everywhere on all surfaces since limited areas on some of the boards were left raw even after the planing. In two of the boards the pith was located within the cross-section. The boards contained both live and dead knots. The dot laser scanning was performed by a high resolution laser scanner of the make WoodEye. The WoodEye also contains an end scanning camera that may be used to determine an approximate location of pith for the first board end leaving the system.

Methods and measurements

Detection of knots on timber surfaces using the tracheid effect

Dot laser scanning using the tracheid effect means that the fibre orientation is determined with a certain resolution across flatwise and edgewise board surfaces. The resolution was in this study set to 1 mm in the longitudinal direction and 4 mm in the transverse direction. To create smooth transitions between local dot laser observations a moving average of 5×5 mm^2 was applied to both the in-plane angle and the shape factor ratio determining the value of the diving angle. The latter value was calculated according to Equation (1). The values used for l_1 and l_2 in this equation were set to 0.54 and 0.82 which are the same values as suggested by Olsson and Oscarsson (2014). It should be mentioned that the diving angle could be defined as either positive or negative. For example, if 3D fibre directions determined on wide surfaces of a board are projected to the *yz*-plane, see Figure 2f, then a positive diving angle is assigned to those projected fibre directions that present a positive slope in the *yz*-plane. Consequently, a negative slope results in a negative sign of the mentioned angle. For fibre directions determined on edge surfaces the sign of the angle can be determined in a similar way, but in this case on the basis of projections to the *xy*-plane. A different method for determining the sign of the diving angle is presented in Olsson and Oscarsson (2014). However, for the purposes of this investigation the sign is not important since only the magnitude of deviation between the fibre direction and the longitudinal direction of the board is actually considered.

In order to identify all knots of various types along board surfaces by means of high resolution laser scanning, both the in-plane angle and the diving angle should be considered. To do this a 3D vector, based upon both these angles, was created for each dot laser observation, which means that an assumed local 3D fibre orientation was established for each such observation. Further, by assuming that the pith of the log was parallel with the longitudinal direction of the board, a new local angle between the assumed 3D fibre orientation and the pith of the log was calculated as

$$\varphi = cos^{-1}\left(\frac{u \cdot v}{|u| \cdot |v|}\right) \tag{2}$$

where u and v are the local 3D fibre orientation vector and the pith vector, respectively. All such new local angles (φ) determined over a board's surfaces were then used to identify where the 3D fibre orientation deviated substantially from the pith direction. Such deviations exceeding a set threshold value was interpreted as indications that the dot laser observation belonged to a knot surfaces. On the basis of repeated trials, it was found that an optimum relationship between indicated and actual knot surfaces was achieved for a value of φ equal to 56°. This value was subsequently used as threshold value for determination of both the position of knot surfaces and their corresponding areas on the board's longitudinal surfaces. The practical procedure for subsequent identification of knot surfaces can be summarized as follows; (a) for every dot laser observation the position in the coordinate system was defined by the scanning, (b) by using a binary numbering system, all observations for which the threshold value (56°) was exceeded, the binary value was set to 1, c) all observations which had a binary value equal to 1 and was located next to each other on a board surface was regarded as one coherent knot surface, and (d) even if two such knot surfaces were not located exactly next to each other, but had a distance between the centroids of them that was smaller than

$$r_{crit} = \sqrt{A_1/\pi} + \sqrt{A_2/\pi} \quad (3)$$

where A_1 and A_2 are the areas of the two knot surfaces, the two knot surfaces were considered as a single knot of size $A_1 + A_2$. Figure 2a shows photographs of four longitudinal surfaces of a part of one of the investigated boards. Figure 2b shows colour plots, for the same surfaces, of the calculated angle φ between the assumed fibre orientation in 3D and the direction of the pith. The colour bar describes the angle between the direction of the pith and the assumed fibre orientation; colours from yellow/orange to red implies a large angle, which indicates a knot surface, whereas blue colour means that the angle is small, i.e. indicating clear wood areas. The viewing principle of these figures is that the images can be folded around their longitudinal direction, i.e. the *y*-direction and thus, creating a 3D view of the board. The results displayed in Figure 2b show good resemblance with the actual surfaces of the board shown in Figure 2a.

Three-dimensional modeling of knots

In the following it is described how it can be concluded whether knot surfaces that are visible on different board surfaces are actually parts of the same physical knot. It is common knowledge that branches grow outwards from the pith of the log and usually slightly upwards and it is assumed that the centroid of a knot area correspond to the location of the pith of the branch at a distance r_i from the pith of the log, see Figure 2c. As mentioned in section *Material and equipment*, the WoodEye scanner may be used to determine the location of the pith of the log at the first board end leaving the system. However, due to poor calibration of the end scanning camera in the WoodEye scanner used in this investigation, the described determination of the pith location had to be carried out manually. Having knowledge of an approximate location of the pith of the log (illustrated by the filled circle in Figure 2c), the positions of the centroids of the knot areas identified could be transformed to a polar coordinate system. Then, by comparing the position of two knot surfaces that are visible on different sides of the board, with respect to their tangential and longitudinal coordinates, respectively, it becomes obvious if the two knot surfaces belong to the same physical knot, see Figure 2c. The difference between two tangential coordinates can be denoted $\Delta\theta$, see Figure 2c. Of course, depending on 1) limited accuracy regarding the assumed location of the pith of the log, 2) limited accuracy in the interpretation of knot surfaces 3) limited knowledge regarding the actual growth direction of the branch and 4) misinterpretation of the location of the pith within the knot, *e.g.* because the knot surfaces may be cut off at an edge of the board, some difference in the polar and longitudinal coordinates, i.e. some tolerance that can be expressed as $\Delta\theta_{\text{limit}}$ and Δl_{limit}, respectively, have to be allowed for when comparing tangential coordinates and longitudinal position. Thus it is assumed that two knot surfaces, *i* and *j*, visible on different surfaces, are parts of the same physical knot if

$$|\theta_i - \theta_j| < \Delta\theta_{limit} \quad (4)$$

and

$$|y_i - y_j| < \Delta l_{limit} \quad (5)$$

in which

$$\Delta l_{limit} = a \cdot |r_i - r_j| \quad (6)$$

where $\Delta\theta_{\text{limit}}$ was set to 18.5° and a was set to 0.8. The constant a is dimensionless and can be changed if another species of timber is examined in a similar way. Both these values where set by repeated trial. With knowledge of which knot surfaces that were parts of the same physical knot, it was then possible to model knots in 3D as convex hulls, i.e. with the smallest convex volume that connected the different knot surfaces as shown in Figure 2d–e. Figure 2f shows a complete 3D knot model for a part of one of the investigated board. The four knots with the highest *y*-coordinates correspond to the knots visible in Figure 2a.

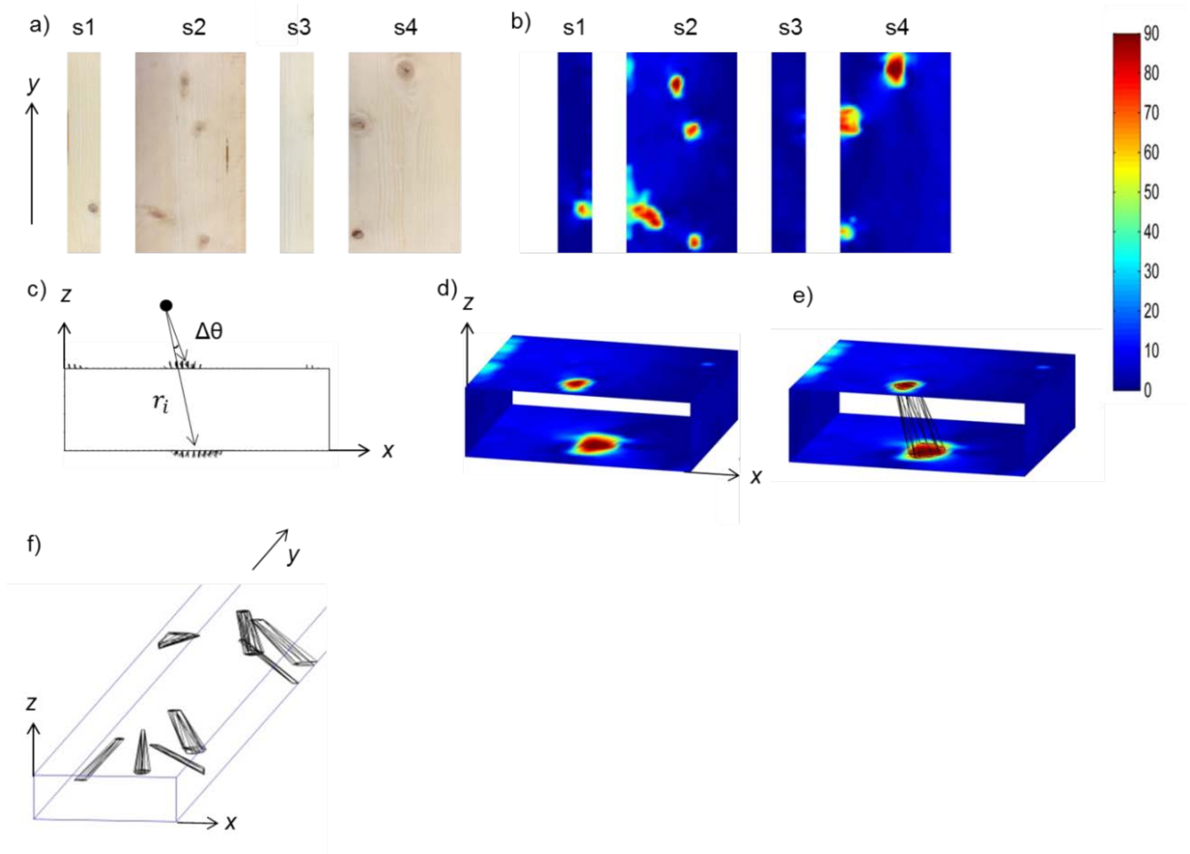

Figure 2—a) Photographs of a part of one of the investigate boards. b) The angle φ between the assumed 3D fibre orientation and the longitudinal direction of the board, for the same surfaces as in (a). The colourbar indicates the size of φ. c) Projection onto the *xz*-plane of the assumed 3D fibre orientation for the uppermost knot shown in (b). The knot is marked on two surfaces and indicated with respect to position with polar coordinates. d) A three dimensional view of the uppermost knot surfaces visible in (b). e) The knot volume inside the board modelled as convex hull. f) A complete 3D knot model for a part of a board. The four knots with the highest *y*-coordinate correspond to the knots visible in (a).

Results and discussion

Validation of identified knot surfaces areas

The ability of the algorithm to determine areas of knot surfaces were verified by manually measuring the knot area on photographs of the board surfaces in the software AutoCAD Architecture. The knot areas measured on photographs and the knot areas assessed by means of the algorithm, for all the knots that are visible on the part of a board that is shown in Figure 2a–b, respectively, are presented in Table 1. In this part of the board there are in total seven round knots, i.e. knots that are cut off in a plane that is fairly close to an *lt*-plane, and one oval knot, i.e. a knot that is cut off in a plane between the *lt*-plane and *lr*-plane. In some photograph, the size of the knot areas is difficult to assess manually since the border between the knot and the surrounding clear wood is fuzzy. Such knots are indicated with an approximately-equal-to sign in Table 1 and the knot area is rounded off to the nearest fiftieth mm^2. The radius given are, for the round knots, simply the square root of the knot area divided by π, and the lengths given for the major- and minor radius of the oval knot were determined manually by approximating the oval knot area with an ellipse of the same size. As shown in Table 1, the radius of the round knots, estimated by means of the algorithm and manually from photographs, respectively, is quite similar. Considering the knots with well-defined boundaries the largest error of the radius is only 2 mm. The mean error of the radius is smaller than 1 mm and it can be concluded that the algorithm that is based on a criterion for the angle between the assessed fibre direction and the direction of the board is able to determine the areas of the knot surfaces accurately.

Table 1—Knot areas measured on photographs and knot areas assessed by means of the proposed algorithm. The knots considered are those of the part of the board that is shown in Figure 2a–b. Numbering starts with the knot having the lowest *y*-coordinate on each side.

Knot no. (side)	Knot type	y-coordinate *(mm)*	Knot area algorithm *(mm^2)*	Knot area photograph *(mm^2)*	Radius round knots		Major and minor radius of elliptically shaped knots			
					Algorithm *(mm)*	Photograph *(mm)*	Algorithm *(mm)*		Photograph *(mm)*	
							Major	Minor	Major	Minor
1 (s1)	Round	1040	99	77	6	5	-	-	-	-
2 (s2)	Round	998	118	114	6	6	-	-	-	-
3 (s2)	Elliptic	1032	616	≈ 350	-	-	19	10	16	7
4 (s2)	Round	1144	181	179	8	8	-	-	-	-
5 (s2)	Round	1204	218	190	8	8	-	-	-	-
6 (s4)	Round	1013	54	93	4	5	-	-	-	-
7 (s4)	Round	1155	616	≈ 400	14	11	-	-	-	-
8 (s4)	Round	1225	670	515	15	13	-	-	-	-

Validation of the 3D knot model

In section *Three-dimensional modelling of knots* it was explained how it can be concluded if knot surfaces that are visible on different surfaces of a board are parts of o the same physical knot, and how 3D models of knots can be established on the basis of such knowledge. A complete 3D model of knots for a part of a board was shown in Figure 2f. An account of the knots identified by means of the proposed algorithm and by manual inspection, respectively, is given in Table 2 for two different boards. The comparison show that all knots with surface areas larger than 100 mm^2 were identified by the algorithm and also that all knots having at least one surface larger than that 100 mm^2 were correctly associated with other surfaces of the same knot. For knot surfaces with areas between 10–100 mm^2 approximately 60 % of them were correctly associated and modeled in 3D by the algorithm. In two cases spots on the board surfaces that were poorly planed were erroneously identified as knot surfaces. This also led to a connection between one such spurious knot surface and a real knot surface which meant that one knot was modelled as a volume in an incorrect manner. The reason why a rough clear wood surface could be identified as a knot is that the laser dots illuminating such a surfaces may display more round shapes than what they would have done on a corresponding planed clear wood surface. The result is, of course, that large diving angles of fibres are incorrectly identified on such surface.

Table 2—An account of knot surfaces and knots in 3D identified by means of the proposed algorithm and by manual inspection, respectively, for board number 7 and board number 9.

Board no.	7		9*	
Knot surface area (*mm^2*)	*10-100*	>100	*10-100*	>100
No. of knot surfaces (determined visually)	40	44	36	50
No. of knot surfaces identified by the algorithm	29	44	19	50
No. of knots in the board (determined visually)	18	14	15	20
No. of knots correctly identified by the algorithm	11	14	8	20
No. of knots incorrectly identified by the algorithm	0	0	1	0

***** One 20 cm long section of board number 9 is excluded due to a large and uncommon defect.

Conclusions and further research

The method used in this paper to identify knots through laser scanning and 3D modelling has proven to work well. For the two boards closely examined all knots with surface areas larger than 100 mm^2 were correctly identified and modelled in 3D. Further, for knots with surfaces between 10–100 mm^2 approximately 60 % were correctly identified and modelled. However, it has also been found that when utilizing the tracheid effect for the purposes of identifying knots it is important that the surfaces are thoroughly planed. Otherwise there is a risk that a poorly planed surface will be identified as a knot surfaces. A limitation of the described method for 3D modelling of knots is that it only works when the pith of the log is placed outside the cross-section.

Reference list

Boughton, G. (1994) *Superior sorting of timber using localized stiffness on edge.* In: Proceedings of the Pacific Timber Engineering Conference, Gold Coast, Australia, July 11–15.

Dynalyse AB (2015) Precigrader. http://dynalyse.se/precigrader/ (2 June 2015).

Foley, C. (2003) *Modeling the effect of knots in structural timber.* Doctoral thesis, Division of Structural Engineering, Report TVBK-1027, Lund Institute of Technology, Lund, Sweden

Hoffmeyer, P. (ed.) (1995) *Styrkesortering ger mervärde, Del 2 – Tillgaengelig teknik (Strength grading adds value, Part 2 – Available technique).* Laboratoriet for Bygningsmaterialer, Danmarks Tekniske Universitet, Teknisk Rapport 335-1995, ISSN 0908-3871 (in Danish, Norwegian and Swedish).

Innovativ Vision (2015) WoodEye. http://woodeye.se/ (18 June 2015).

Johansson, C.-J. (2003) *Grading of timber with respect to mechanical properties.* In: Thelandersson, S. and Larsen, H. J. (eds.) *Timber engineering,* John Wiley & Sons, Chichester, England, pp. 23–43.

Olsson, A., Oscarsson, J., Serrano, E., Källsner, B., Johansson, M., Enquist, B. (2013) *Prediction of timber bending strength and in-member cross-sectional stiffness variation on the basis of local wood fibre orientation.* European Journal of Wood and Wood Products, 71(3):319–333.

Olsson, A., Oscarsson, J. (2014) *Three dimensional fibre orientation models for wood based on laser scanning utilizing the tracheid effect.* In: World Conference on Timber Engineering, Quebec City, Canada, August 10–14.

Oscarsson, J., Olsson, A., Enquist, B. (2014) *Localized modulus of elasticity in timber and its significance for the accuracy of machine strength grading*. Wood and Fiber Science, 46(4):489−501.

Petersson, H. (2010) *Use of optical and laser scanning techniques as tools for obtaining improved FE-input data for strength and shape stability analysis of wood and timber.* In: 5th European Conference on Computational Mechanics, Paris, France, May 16–21.

Shigo, A. L. (1997) *A new tree biology; facts photos and philosophies on trees and their problems and proper care.* Eighth printing. Shigo and Trees, Associates. Durham, NE, U.S.

Simonaho, S.-P., Palvianien, J., Tolonen, Y., Silvennoinen, R. (2004) *Determination of wood grain direction from laser light scattering pattern.* Optics and Lasers in Engineering, 41:95–103.

Åstrand, E. (1996) *Automatic inspection of sawn wood.* Dissertation No. 424, Department of Electrical Engineering, Linköping University, Sweden.